

Point-to-Point trajectory planning of flexible redundant robot manipulators using genetic algorithms

Shigang Yue*,^a Dominik Henrich*, W. L. Xu† and S. K. Tso‡

(Received in Final Form: October 17, 2001)

SUMMARY

The paper focuses on the problem of point-to-point trajectory planning for flexible redundant robot manipulators (FRM) in joint space. Compared with irredundant flexible manipulators, a FRM possesses additional possibilities during point-to-point trajectory planning due to its kinematics redundancy. A trajectory planning method to minimize vibration and/or executing time of a point-to-point motion is presented for FRMs based on Genetic Algorithms (GAs). Kinematics redundancy is integrated into the presented method as planning variables. Quadrinomial and quintic polynomial are used to describe the segments that connect the initial, intermediate, and final points in joint space. The trajectory planning of FRM is formulated as a problem of optimization with constraints. A planar FRM with three flexible links is used in simulation. Case studies show that the method is applicable.

KEYWORDS: Redundancy; Flexible-link robot; Trajectory planning; Point-to-point; Vibration; Genetic algorithms

1. INTRODUCTION

The use of a light-weight flexible robotic manipulator can increase the load carrying capacity and the operational speed. Other potential advantages of flexible robot include lower energy consumption, use of smaller actuators, safer operation due to reduced inertia, easier transport, and a more compliant structure for assembly. Much work performed on flexible robot manipulators in past decades involve mainly modeling and vibration- and trajectory tracking control.^{1–3} Since most of the robot tasks cannot be conducted without maintaining a certain accuracy, the key problem of flexible robot manipulators is the reduction in the endpoint's error resulting from vibration. This vibration remains even after the robot arm reached the goal.

Several different approaches have already been reported and proven to be applicable for reducing vibrations of one- or two-link flexible arms. Most of the work is based on (either open-loop or closed-loop) control strategies. For

example, Mohri et al.⁴ developed a planning method with reduced vibration for a two link flexible manipulator along a specified path, Singer et al.⁵ and Singhose et al.⁶ presented shaping techniques to reduce robot arm vibration, Choura et al.⁷ presented an open-loop control method for a rotating flexible beam, while Hillsley and Yurkovich⁸ compared the feedback control, shaping techniques and the composite control method for a two-link flexible robot arm. However, the above research focussed on flexible robot manipulators with only one or two links.

It has been found recently that the redundancy, which is used in robot manipulators to achieve additional performance while tracking a given end-effector trajectory,^{9,10} has a special application in vibration reduction of flexible manipulators. Nguyen and Walker¹¹ made use of the self-motion to compensate for and damp out flexible deformation when the degrees of redundancy are the same as the number of deformation modes to be controlled. Yue¹² presented an optimal method, in which joint flexibility is also taken into account, to choose the self-motion for vibration reduction in FRM. Kim and Park¹³ employed the self-motion capability to solve the tracking control problem of a FRM, and developed an algorithm in which the self-motion is evaluated so as to nullify the dominant modal force of flexural motion induced by a rigid body motion. Nevertheless, trajectory planning of FRM in joint space was not mentioned in the above papers.

Recently, research has been performed in new domains of advanced robotics, i.e. large redundant robots with special application fields, for example, aircraft cleaning and removing paint from hulls. Off-line motion programs which satisfy time and energy optimization criteria are developed while considering compensation for the displacement caused by the deflection of a large redundant robot.^{14,15}

Compared with one- or two-link flexible robot manipulators, it is reasonable to expect that kinematics redundancy can also provide additional possibilities to minimize vibration and/or execution time for FRMs by performing trajectory planning in joint space. Moreover, the geometric problems with Cartesian paths related to workspace and singularities can be avoided if the point-to-point task is planned in joint space. Even for large redundant robots mentioned above, an appropriate trajectory with acceptable vibration can save displacement compensation computing time.

Genetic Algorithms (GAs) are population-based, stochastic, and global search methods. Their performance is superior to that of classical techniques^{16,17} and they have been used successfully in robot path planning.^{18,19} As

* Embedded Systems and Robotics (RESY), Informatics Faculty, University of Kaiserslautern, D-67653 Kaiserslautern (Germany). E-mail: [shigang, henrich]@informatik.uni-kl.de. Website: <http://resy.informatik.uni-kl.de/>

^a Research Fellow of the Alexander von Humboldt Foundation, from Beijing Polytechnic University.

†Institute of Technology and Engineering, Massey University, Palmerston North (New Zealand).

‡Center for Intelligent Design, Automation and Manufacturing, City University of Hong Kong, Kowloon (Hong Kong).

discussed in, references [9, 10] a global solution is quite difficult to achieve using traditional methods. The global search ability of GAs provides a possibility to find global solutions of redundancy. There has been little reported work on applying GAs to trajectory planning for flexible robot manipulators.

In the following chapters, a trajectory planning method for FRM, based on Genetic Algorithms to minimize vibration and/or executing time while moving between the initial and final points, is presented. First, a finite element model for describing FRM dynamics is introduced (Section 2). Kinematics redundancy is integrated into the planning method as variables (Section 3). Quadrinomial and quintic polynomial are used to describe the paths which connect the initial, intermediate and final points in joint space (Section 4). The trajectory planning for FRM is formulated as a problem of optimization (Section 5). Suitable parameters for each polynomial between two points and suitable initial and final configurations are determined using GAs (Section 6). Finally, a planar FRM with three flexible links is used in simulations, and two case studies are conducted and discussed (Section 7).

2. DYNAMIC MODEL OF FRM

The finite element method is employed to build up the dynamics equations of a FRM with multiple flexible links. Figure 1 shows a generalized deformable element used here with eight parameters. The transverse deflections of the element are modeled by a quintic polynomial and the longitudinal deflections assumed to be a linear polynomial.²⁰ The coordinates of the element are assembled in a vector form as;

$$\vec{\phi}_e = (\phi_1 \quad \phi_2 \quad \cdots \quad \phi_8)^T \quad (1)$$

where ϕ_1 and ϕ_5 are the axial displacements along the x -axis, ϕ_2 and ϕ_6 are the transverse displacements along the y -axis, ϕ_3 and ϕ_7 are the rotary displacements about the z -axis, and ϕ_4 and ϕ_8 are the curvature displacements in the xy plane.

Without taking into account the joint flexibility, the flexible deformations of the robot can be described by system generalized coordinates²⁰ in a matrix form as;

$$\{\Phi\} = \{\Phi_1 \quad \Phi_2 \quad \cdots \quad \Phi_{n_u}\}^T \quad (2)$$

where n_u denotes the total number of the generalized coordinates, and Φ_i represents the i^{th} system generalized coordinates. The dynamic equations of a flexible robot manipulator system can then be written as;

$$[M]\{\ddot{\Phi}\} + [C]\{\dot{\Phi}\} + [K]\{\Phi\} = \{P\} \quad (3)$$

$$\{\tau\} = ([D] + [J_z])\{\ddot{q}\} + \{H\} + \{E\} \quad (4)$$

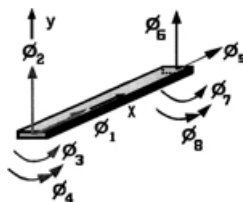


Fig. 1. An element and its generalized coordinates.

where $[M]$ is the $n_u \times n_u$ global mass matrix, $[C]$ is the $n_u \times n_u$ global damping matrix, $[K]$ is the $n_u \times n_u$ global stiffness matrix, $\{P\}$ is the $n_u \times 1$ inertia force matrix, $\{\dot{\Phi}\}$ and $\{\ddot{\Phi}\}$ are the generalized velocity vector and generalized acceleration vector respectively, which describe the deformation behavior of the flexible links, n_u is the number of the coordinates, $[D]$ is the $n \times n$ inertia mass matrix, $\{q\}$ and \ddot{q} are, respectively, the vectors which describe the joint angle and angular acceleration, $\{H\}$ is the $n \times 1$ centrifugal, gravitational coriolis of rigid and flexible coupling terms, $\{E\}$ is the $n \times 1$ link flexibility term, $[J_z]$ is the $n \times 1$ rotor inertia mass matrix, $\{\tau\}$ is the $n \times 1$ actuator torque matrix, and n is the number of joints in the robot system. All the matrices above are functions of $\{q\}$, $\{\dot{q}\}$ and $\{\ddot{q}\}$.

3. REDUNDANCY RESOLUTION OF A FRM

For a redundant robot, the number of degrees of freedom n of a manipulator is greater than the number of end-effector degrees of freedom m . That is, given a position/posture of the end-effector, there are an infinite number of robot configurations available. In this study, the redundancy of a robot is used to avoid the acute vibration and/or minimize executing time when its end-effector moves from one point to another. How should the redundancy of the FRM be used to attain additional aims, such as to avoid acute vibration? There already exist different methods, so it is useful to introduce the known methods briefly before presenting our own method.

3.1. Real position method

As far as the FRM is concerned, the real pose of its end-effector is the function not only of the joint angle vector $\{q\}$, but also the flexible link deformation;

$$\{x\} = f(q, \theta_f) \quad (5)$$

where $\{x\} \in R^m$ are the coordinates of the end-effector, $\{\theta_f\} \in R^l$ are the coordinates describing the flexible link deformations, and l is the number of the generalized coordinates. Based on the above equations, one may finally obtain the joint planning equations,^{11,12}

$$\begin{aligned} \{\ddot{q}\} = & [J_r^+](\{\ddot{x}\} - [\dot{J}_r]\{\dot{q}\} - [J_f]\{\ddot{\theta}_f\} - [\dot{J}_f]\{\dot{\theta}_f\}) \\ & + ([I] - [J_r^+][J_r])\{\ddot{\epsilon}\} \end{aligned} \quad (6)$$

where $[J_r] \in R^{m \times n}$ is the Jacobian matrix, and $[J_f] \in R^{n \times l}$ is the flexible Jacobian matrix, $[J_r^+] \in R^{n \times m}$ is the pseudoinverse of the Jacobian matrix $[J_r]$, $\{\dot{x}\}$ is the end-effector velocity, $\{\ddot{x}\}$ is the end-effector acceleration, $\{\dot{\theta}_f\}$ is the velocity of the coordinates, $[I] \in R^{n \times n}$ is the unit matrix, $\{\ddot{\epsilon}\} \in R^n$ is the null space vector for the redundant robot, and $([I] - [J_r^+][J_r])\{\ddot{\epsilon}\} \in N(J)$ is the homogeneous solution that is orthogonal with respect to $[J_r^+]\{\dot{x}\}$. The homogeneous solution is the self-motion between the links of a redundant manipulator that does not cause any movement of its end-effector. Furthermore, $[J_r^+]$ is given as;

$$[J_r^+] = [J_r]^T([J_r][J_r]^T)^{-1} \quad (7)$$

Based on equation (6), different self-motions can be chosen according to different demands. The planning equation (6) can also compensate for the flexible deformation automat-

ically. However, this compensation may cause acute vibration due to its high frequency. Moreover, if the vibration deformation can be reduced enough in the later path planning, the compensation becomes unnecessary. Therefore, compensation equation (6) seems to be unpractical for our point-to-point task.

3.2. Nominal position method

The vibration of each point usually occurs around its nominal position, implying that a FRM can be treated as a rigid body robot in certain cases. The nominal position of a rigid redundant FRM can be determined by the joint angle vector $\{q\}$, which means the values of $\{\hat{\theta}_r\}$ and $\{\hat{\theta}_f\}$ in equation (6) are zero. The nominal motion of a FRM can be described as,^{9,10}

$$\{\ddot{q}\} = [J_r^+](\{\ddot{x}\} - [\dot{J}_r]\{\dot{q}\}) + ([I] - [J_r^+][J_r])\{\ddot{\varepsilon}\} \quad (8)$$

The trajectory of a FRM can be planned as for a rigid body robot according to equation (8). It is found that the above method is only applicable when the prescribed trajectory is described by $\{\ddot{x}\}$. This kind of endpoint trajectory, with a Cartesian position and orientation as a function of time, is difficult to generate, especially when a complex type of line is involved.²¹

3.3. Initial and final postures of FRM

The point-to-point trajectory planning can be conducted by using the above equation (6) with compensation or equation (8) without any compensation. However, the results based on equation (6) or (8) are local solutions^{9,10,12} and are prone to various problems related to workspace and singularities, since the trajectory is given in a Cartesian space. As mentioned above, the presented method will conduct the planning problem for the FRM in joint space. This means that the various problems encountered in a Cartesian space can be easily avoided.

Since only a point-to-point trajectory is considered in this paper, there are only two important points (i.e. the initial and final point of a possible path) that should be achieved. Corresponding to the two points, there are infinite possible configurations for each point due to kinematics redundancy, as shown in Figure 2. This means the FRM can start from

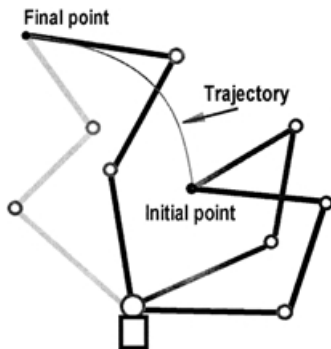


Fig. 2. Different configurations of a FRM correspond to initial and final point of trajectory.

different poses and end with different poses according to its task.

Thus, the redundancy problem with respect to initial and final points is the determination of the initial and final postures. These two postures can be described by $2(n-m)$ parameters in joint space, where $(n-m)$ are the redundant degree of freedom of the FRM. In our approach, as described in the following chapters, these $2(n-m)$ variables can be determined by optimization; thus, the redundancy solution corresponding to initial and final points will be determined by using GAs.

The problems of redundancy corresponding to intermediate via points will also be solved efficiently by planning in joint space instead of in a Cartesian task space, as described in the following sections.

4. TRAJECTORY PLANNING STRATEGY

Here, trajectory refers to a time history of position, velocity, and acceleration for each degree of freedom. Suppose that the point-to-point trajectory is connected by several segments with continuous acceleration at the intermediate via point (as shown in Figure 3). The position of each intermediate point is supposed to be unknown in the following section of the paper. Of course, the intermediate points can also be given as particular points that should be passed through. This is useful especially when there is an obstacle in the working area.

If we wish to be able to specify the position, velocity, and acceleration at the beginning and end of path segment, a quadrinomial and quintic polynomial are required. Let us assume that there are m_p intermediate via points between the initial and the final points.

Between the initial point to m_p intermediate via points, a quadrinomial is used to describe these segments as;

$$\theta_{i,i+1}(t) = a_{i0} + a_{i1}t_i + a_{i2}t_i^2 + a_{i3}t_i^3 + a_{i4}t_i^4, \quad (i=0, \dots, m_p-1) \quad (9)$$

where the constrains are given as

$$\theta_i = a_{i0} \quad (10)$$

$$\theta_{i+1} = a_{i0} + a_{i1}T_i + a_{i2}T_i^2 + a_{i3}T_i^3 + a_{i4}T_i^4 \quad (11)$$

$$\dot{\theta}_i = a_{i1} \quad (12)$$

$$\dot{\theta}_{i+1} = a_{i1} + 2a_{i2}T_i + 3a_{i3}T_i^2 + 4a_{i4}T_i^3 \quad (13)$$

$$\ddot{\theta}_i = 2a_{i2} \quad (14)$$



Fig. 3. Intermediate points on the point-to-point path.

where T_i is the executing time from point i to point $i+1$. The five unknowns can be solved as

$$a_{i0} = \theta_i \quad (15)$$

$$a_{i1} = \dot{\theta}_i \quad (16)$$

$$a_{i2} = \frac{\ddot{\theta}_i}{2} \quad (17)$$

$$a_{i3} = \frac{(4\theta_{i+1} - \dot{\theta}_{i+1}T_i - 4\theta_i - 3\dot{\theta}_iT_i - \ddot{\theta}_iT_i^2)}{T_i^3} \quad (18)$$

$$a_{i4} = \frac{\left(\dot{\theta}_{i+1}T_i - 3\theta_{i+1} + 3\theta_i + 2\dot{\theta}_iT_i + \frac{\ddot{\theta}_iT_i^2}{2}\right)}{T_i^4} \quad (19)$$

The intermediate point $i+1$'s acceleration can be obtained as:

$$\ddot{\theta}_{i+1} = 2a_{i2} + 6a_{i3}T_i + 12a_{i4}T_i^2 \quad (20)$$

The segment between the number m_p of intermediate points and the final point can be described by quitic polynomial as;

$$\theta_{i,i+1}(t) = b_{i0} + b_{i1}t_i + b_{i2}t_i^2 + b_{i3}t_i^3 + b_{i4}t_i^4 + b_{i5}t_i^5, (i=m_p) \quad (21)$$

where the constraints are given as;

$$\theta_i = b_{i0} \quad (22)$$

$$\theta_{i+1} = b_{i0} + b_{i1}T_i + b_{i2}T_i^2 + b_{i3}T_i^3 + b_{i4}T_i^4 + b_{i5}T_i^5 \quad (23)$$

$$\dot{\theta}_i = b_{i1} \quad (24)$$

$$\dot{\theta}_{i+1} = b_{i1} + 2b_{i2}T_i + 3b_{i3}T_i^2 + 4b_{i4}T_i^3 + 5b_{i5}T_i^4 \quad (25)$$

$$\ddot{\theta}_i = 2b_{i2} \quad (26)$$

$$\ddot{\theta}_{i+1} = 2b_{i2} + 6b_{i3}T_i + 12b_{i4}T_i^2 + 20b_{i5}T_i^3 \quad (27)$$

and these constraints specify a linear set of six equations with six unknowns whose solution is;

$$b_{i0} = \theta_i \quad (28)$$

$$b_{i1} = \dot{\theta}_i \quad (29)$$

$$b_{i2} = \frac{\ddot{\theta}_i}{2} \quad (30)$$

$$b_{i3} = \frac{(20\theta_{i+1} - 20\theta_i - (8\dot{\theta}_{i+1} + 12\dot{\theta}_i)T_i - (3\ddot{\theta}_i - \ddot{\theta}_{i+1})T_i^2)}{2T_i^3} \quad (31)$$

$$b_{i4} = \frac{(30\theta_i - 30\theta_{i+1} + (14\dot{\theta}_{i+1} + 16\dot{\theta}_i)T_i + (3\ddot{\theta}_i - 2\ddot{\theta}_{i+1})T_i^2)}{2T_i^4} \quad (32)$$

$$b_{i5} = \frac{(12\theta_{i+1} - 12\theta_i - (6\dot{\theta}_{i+1} + 6\dot{\theta}_i)T_i - (\ddot{\theta}_i - \ddot{\theta}_{i+1})T_i^2)}{2T_i^5} \quad (33)$$

As formulated above, the total parameters to be determined are the joint angles of each intermediate via point ($n \times m_p$ parameters), the joint angular velocities of each intermediate point ($n \times m_p$ parameters), the execution time for each segment ($m_p + 1$ parameters), and the initial and final posture of the FRM ($2(n - m)$ parameters). Therefore, there are a total of $((2n + 1)m_p + 2(n - m) + 1)$ parameters to be determined. It should be pointed out that the joint angular acceleration at each intermediate point can be obtained via equation (20). If all the intermediate points are connected by quintic polynomials, there will be $((3n + 1)m_p + 2(n - m) + 1)$ parameters to be determined. This would be more time-consuming, that is why we choose both quadrinomial and quintic polynomial to generate the segments.

All of the above parameters can be determined by using the following optimization method.

5. OPTIMIZING THE TRAJECTORY USING GAS

For a point-to-point trajectory planning problems of FRM, the vibrational deformation amplitude is one of the most important factors involved in the optimization. It is reasonable to assume the vibration deformation amplitude as one of the objects in the path planning process.

$$f = a_{vib} \quad (34)$$

where a_{vib} is the largest amplitude of vibrational deformation during the point-to-point path. The above optimization is available only when the execution time from one point to another is fixed or prescribed.

Therefore, it is also obvious that the total execution time is another important factor that has a significant influence on the dynamic behaviors of a FRM. Thus, a multiple objective optimization is presented. Equation (34) can be extended as;

$$f_m = w_1 a_{vib} + w_2 t_{ptp} \quad (35)$$

where w_1 and w_2 are the weight coefficients and t_{ptp} is the total execution time for the point-to-point motion of a FRM.

Since the limitations of joint angles, joint angular velocities, joint angular accelerations and joint torques are considered in the optimal process, the objective and constraints are finally written as;

$$\min \rightarrow f_m = w_1 a_{vib} + w_2 t_{ptp} \quad (36)$$

$$s.t. \quad q_{i,\min} \leq q_i \leq q_{i,\max} \quad (i = 1, \dots, n) \quad (37)$$

$$\omega_{i,\min} \leq \omega_i \leq \omega_{i,\max} \quad (i = 1, \dots, n) \quad (38)$$

$$\varepsilon_{i,\min} \leq \varepsilon_i \leq \varepsilon_{i,\max} \quad (i = 1, \dots, n) \quad (39)$$

$$T_{i,\min} \leq T_i \leq T_{i,\max} \quad (i = 1, \dots, m_p) \quad (40)$$

$$\tau_{i,\min} \leq \tau_i \leq \tau_{i,\max} \quad (i = 1, \dots, n) \quad (41)$$

where $q_{i,\min}$ and $q_{i,\max}$ are the lower and upper permitted angle of the i^{th} joint, $\omega_{i,\min}$ and $\omega_{i,\max}$ are the lower and upper permitted angular velocities of the i^{th} joint, $\varepsilon_{i,\min}$ and $\varepsilon_{i,\max}$

```

Procedure ptp
BEGIN
  N:=0;
  Initialize ( $P_N$ );
  Evaluate ( $P_N$ );
  REPEAT
    Selection parents from  $P_N$ ;
    Crossover ( $P_N$ );
    Mutation ( $P_N$ );
    Form new generation  $P_N$ ;
    Evaluate ( $P_N$ );
    N:=N+1;
  UNTIL Termination Condition = True;
  Select point-to-point trajectory of FRM;
END

```

Fig. 4. Procedure to optimize point-to-point trajectory of FRM.

are the lower and upper permitted angular accelerations of the i^{th} joint, $T_{i,min}$ and $T_{i,max}$ are the lower and upper permitted executing times of the i^{th} segment, and $\tau_{i,min}$ and $\tau_{i,max}$ are the lower and upper computed torque of the i^{th} joint, respectively.

Since the basic formulation of point-to-point motion is given, if the parameters of the motion have been determined, then the optimal trajectory can be easily determined. We use genetic algorithms to determine those parameters. GA programs can be found described in detail.¹⁷ The GA procedure proposed to optimize point-to-point trajectories of FRM is shown in Figure 4.

In the procedure, the coding method for the parameters is binary coding, which has been shown to be the most effective coding method for this type of parameter optimization.¹⁷

As shown in Figure 4, initialization randomly generates an initial host population P_0 . The population P_N of the N^{th} generation is formed by survivors from the last generation and new individuals generated through mutation and crossover. Single-point crossover is used to form the new generation. The point-to-point trajectory is finally decided when the termination condition is satisfied. The termination condition of the procedure can be maximum generations or a certain value according to different demand.

Table I. The robot parameters involved in simulation

Length of each link	250 mm
Height of each link	3 mm
Width of each link	4 mm
Elastic modulus	7.10×10^{10} Pa
Shear modulus	2.60×10^{10} Pa
Lumped mass at each distal end of link	40 g
Lumped mass at endpoint	20 g
Moment inertia of base joint	1.5×10^{-5} Kg m^2
Moment inertia of 2 nd joint	1.0×10^{-5} Kg m^2
Moment inertia of 3 rd joint	0.5×10^{-5} Kg m^2

6. CASE STUDIES

A planar FRM with three flexible links is used for the numerical simulation in case studies, as shown in Figure 2. The robot has one redundant degree of freedom in terms of positioning. Its parameters are given in Table 1). The materials of each link is aluminum. All of the cases are simulated in the horizontal plane with no obstacle in the working area.

The constraints used in the following cases are: joint angles $q_i \in [-2\pi, 2\pi]$ rad, joint angular velocities $\omega_i \in [-8, 8]$ rad/s, joint angular accelerations $\varepsilon_i \in [-40, 40]$ rad/s², computed joint torques $\tau_1 \in [-2.5, 2.5]$ Nm, $\tau_2 \in [-1.5, 1.5]$ Nm, and $\tau_3 \in [-1.0, 1.0]$ Nm respectively.

6.1. Case one

In this case study, only the vibrational amplitude is assumed to be the objective of optimization. One intermediate via point and a one second execution time for each segment are assumed, while the termination condition of 200 generations was used. All the selected trajectories start from the same initial configuration. There are seven parameters to be determined in this case, viz. configuration at final point, the three joint angles and the three joint angular velocities of the intermediate point. The optimal process costs about a half hour with a Pentium II computer. The results are below.

It is found that the vibrational amplitude is obviously reduced (shown in Figure 5. Vibration at different genera-

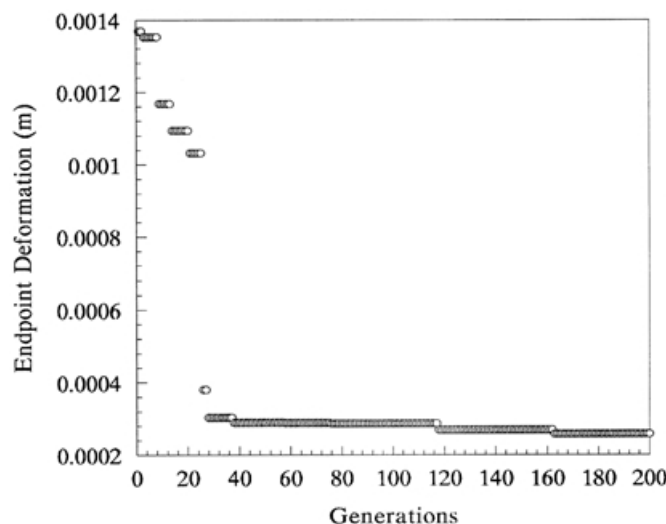


Fig. 5. Endpoint deformation amplitude of FRM versus number of generations.

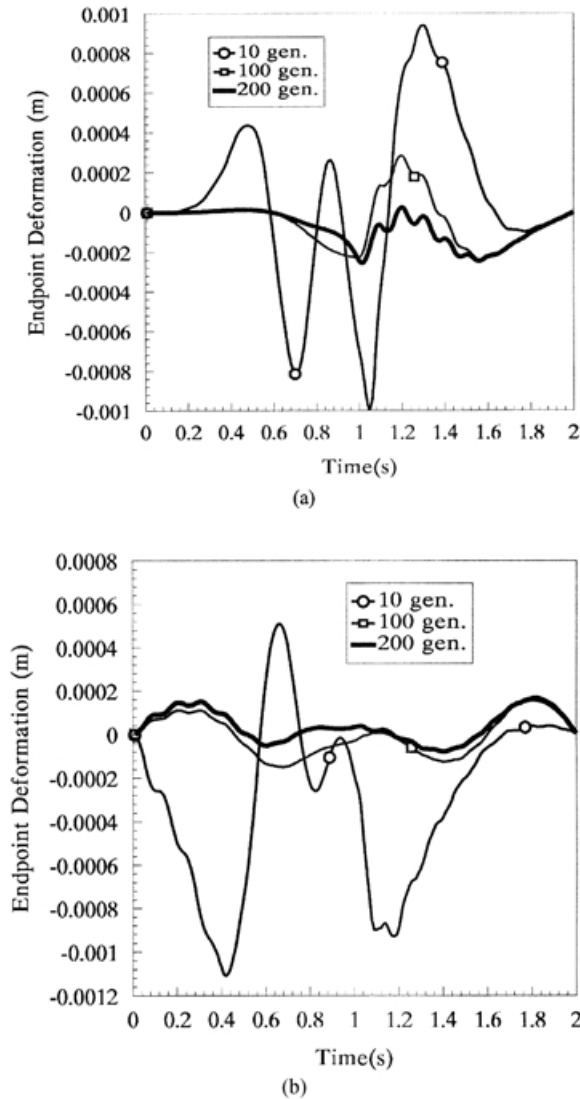


Fig. 6. Endpoint deformation curves at 10th, 100th and 200th generations (a) in x direction (b) in Y direction respectively.

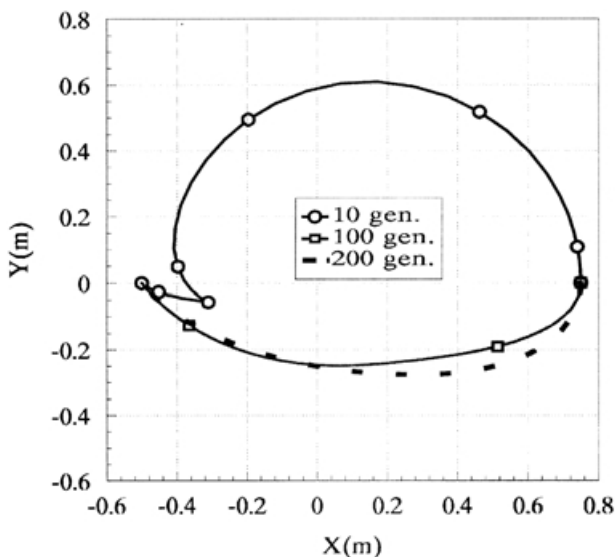


Fig. 7. The end-effector's trajectory at 10th, 100th and 200th generations (The point-to-point paths start from right to left).

tions can be found in detail in Figure 6. The end-effector's trajectories between the two points are shown in Figure 7. It is noticeable that the end-effector's trajectories are quite different between the 10th and 100th generations (Figure 7). The vibrational amplitude decreased rapidly between these generations, reflecting the ability of GAs to find solutions with efficiency.

The joint angle, angular velocity, angular acceleration and computed joint torque of each joint at the 10th, 100th and 200th generation are compared in Figures 8, 9 and 10, respectively. It is clear that the first and second joint angular acceleration at the 100th or 200th generation is quite smooth, however, the third joint angular acceleration at the same generation has a sharp peak. This means that the third link swings to avoid acute inertia. Since the computed torque can be influenced by vibration, the results at different generations are also quite different, even at the end of trajectories (as shown in Figure 10).

The configurations at the 10th, 100th and 200th generations are shown in Figure 11. It was found that the 100th and 200th generation's moving areas are confined to one side and have

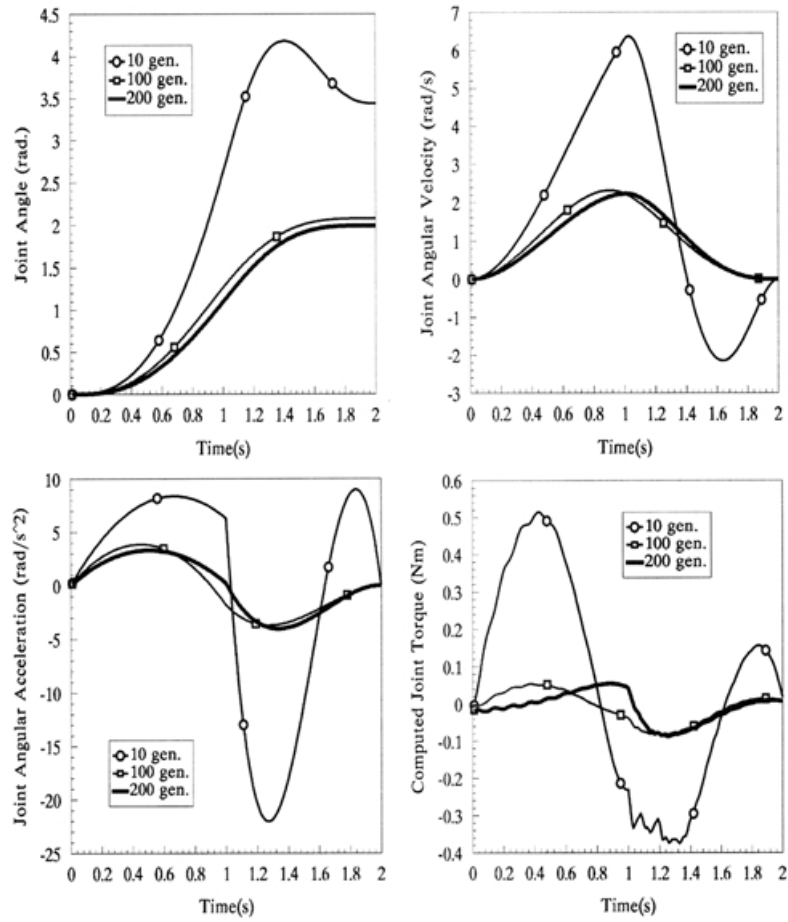


Fig. 8. The angle, angular velocity, angular acceleration and computed joint torque of the first joint at 10th, 100th and 200th generation.

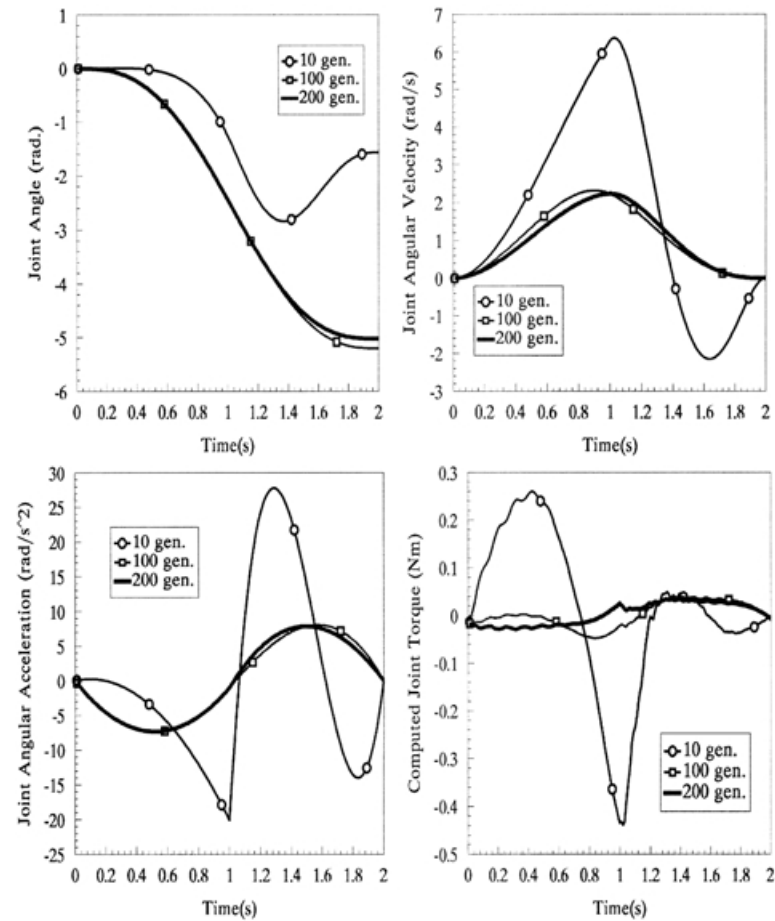


Fig. 9. The angle, angular velocity, angular acceleration and Computed joint torque of the second joint at 10th, 100th and 200th generation.

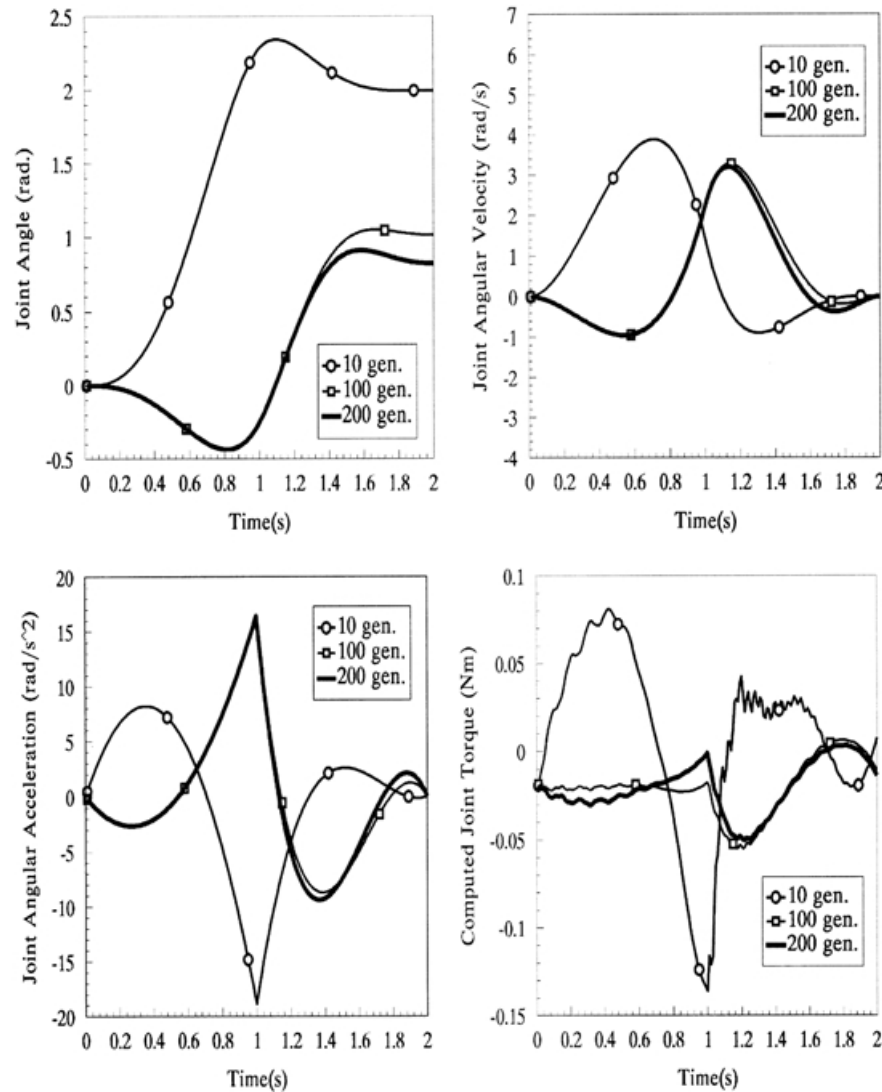


Fig. 10. The angle, angular velocity, angular acceleration and Computed joint torque of the third joint at 10th, 100th and 200th generation.

shorter trajectories compared with the 10th generation. However, the straight line from the initial to the final point, while the shortest one, is far from the best one according to the GA optimization results.

6.2. Case two

In case two, the execution time for the two segments and the vibrational amplitude are both assumed to be part of the objective, according to equation (36).

The multiple weighted value is, in fact, acting as the fitness. The weight coefficient w_1 for the vibrational amplitude is assumed to be 100, and w_2 for the execution time is assumed to be 1 during the process. One intermediate via point is also assumed. There are nine parameters to be determined in this case: configuration at final point, the three joint angles and the three joint angular velocities of the intermediate point, and the two execution times for the two segments. All of the selected trajectories start from the same initial configuration.

The results can be found in the following figures. Figure 12 shows the multiple weighted values and the execution time for each segment versus number of generations. The execution time for each segment decreases sharply before the 40th generation. The execution time of the segment was observed to increase a bit around the 30th generation, because other aspects of the multiple objective were reduced in the meantime.

The optimization results at the 40th and 200th generations are compared in detail in Figures 13 through Figure 17. Although the vibrational amplitude and execution time are reduced sharply even after 40 generations, one finds that after 160 generations, each of the parameters is reduced greatly.

One may also find that at the 40th generation, the third joint opens too much at the first segment and has to be closed a little bit at the second segment as shown in Figure 16 and Figure 17. This kind of useless motion may not only increase executing time, but also increase the inertia, which results in vibration. This maybe explains why the 200th

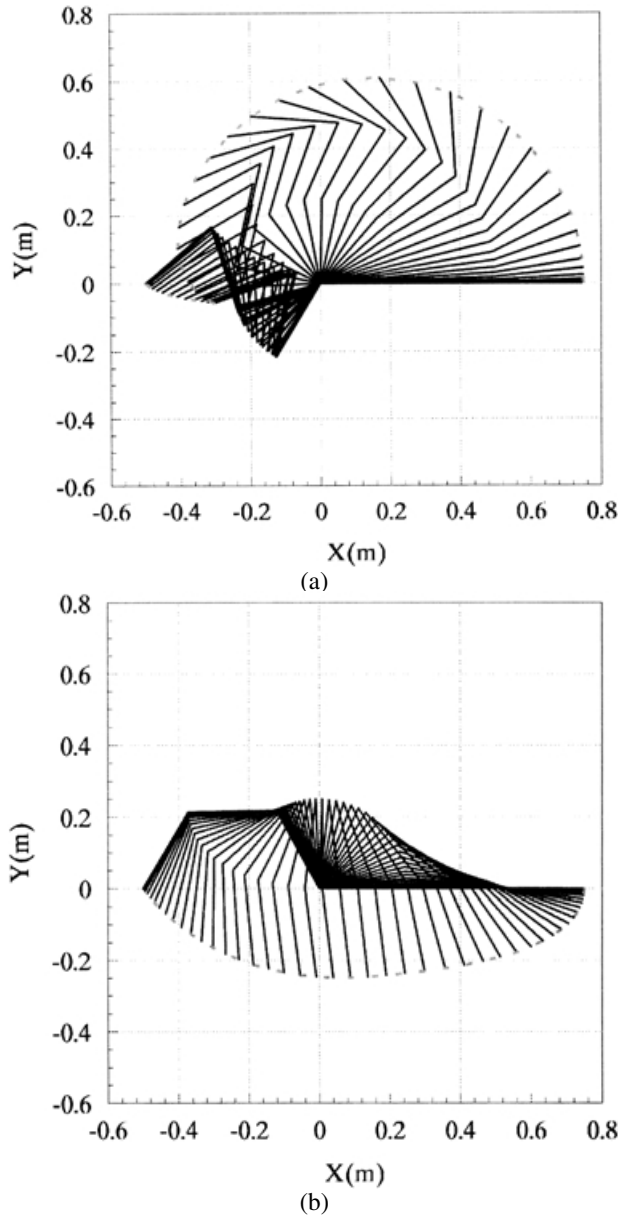


Fig. 11. The configurations of FRM at (a) 10th generation, (b) 100th generation and (c) 200th generation respectively.

generation seems to be more effective in the multiple objective optimization.

As shown in the above two cases, our presented approach for point-to-point trajectory planning of FRMs to minimize vibration amplitude and/or executing time has proven to be applicable. Moreover, special objectives (joint acceleration, torques, etc. for example) can also be integrated into the multiple objective to reach special aims.

It should be noticed that the resolution of robots is not considered in the above planning method. The actual vibration (and, of course, the actual trajectory) may be different, as it would be affected by the actual control torques applied.

7. CONCLUSIONS

In the above sections, the problem of trajectory planning for FRMs is studied in detail. A trajectory planning method for FRM based on Genetic Algorithms (GAs) to minimize

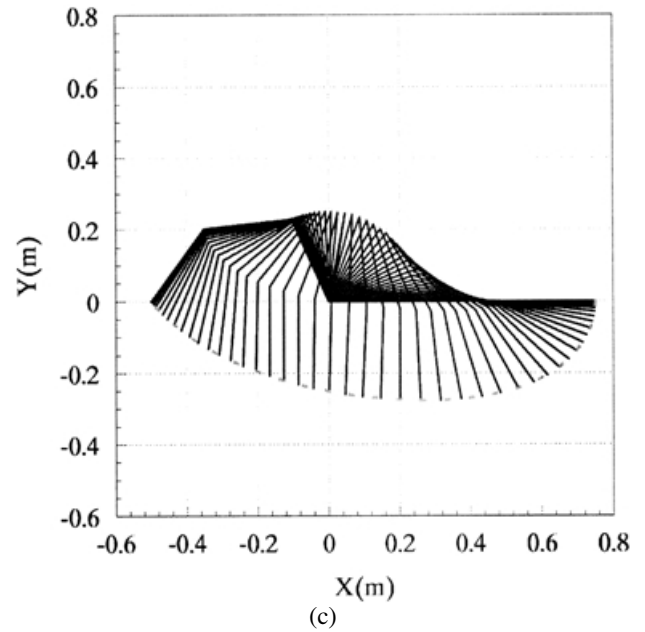


Fig. 11. Continued.

vibration and/or executing time of the point-to-point motion is presented. Kinematics redundancy is considered as a planning variable in the presented method. Quadrinomial and quintic polynomials are used to describe the segments that connect the initial, intermediate, and final points in joint

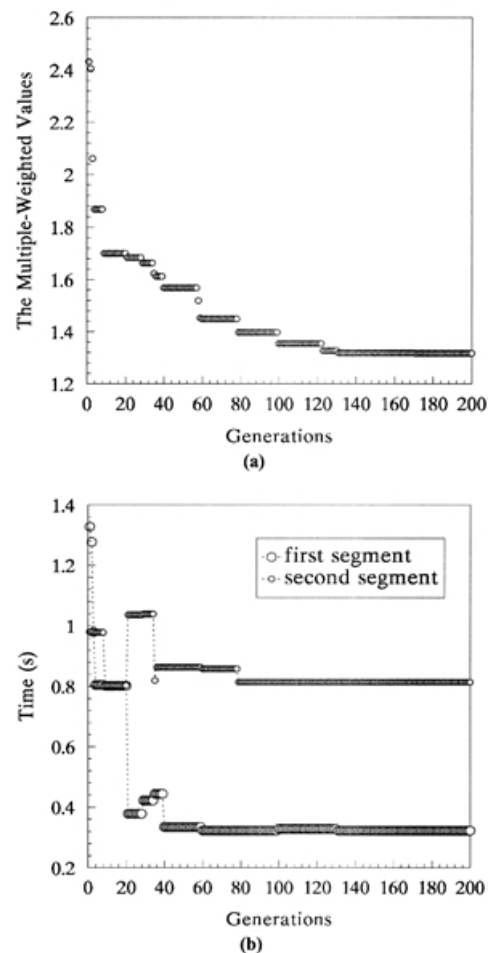


Fig. 12. Multiple weighted value (a) and executing time of each segment (b) versus number of generations.

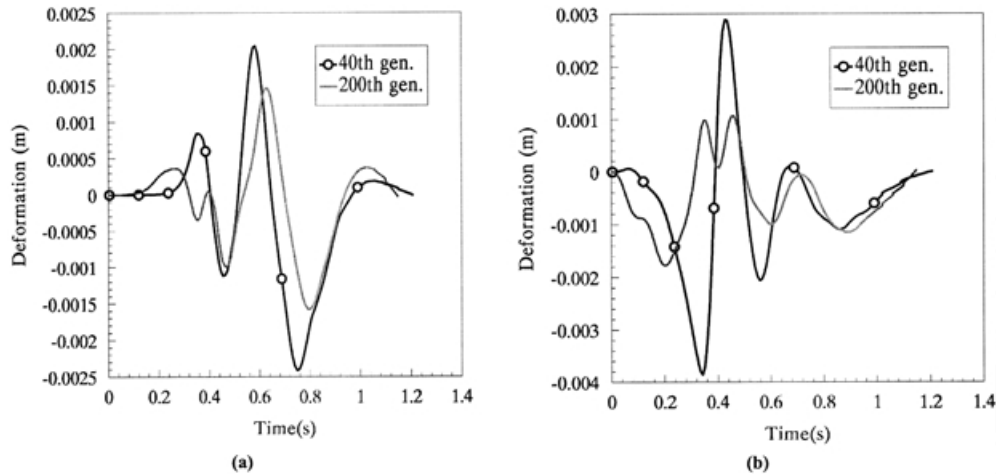


Fig. 13. Endpoint deformation curves in (a) X direction (b) Y direction.

space. Suitable parameters for each polynomial between two points and suitable initial and final configurations can be determined by using GAs. Various problems related to workspace and singularities in Cartesian space are avoided by planning in joint space. A planar FRM with three flexible links was used in simulations. Case studies show the method to be applicable.

The presented approach can be easily extended by integrating additional parameters (for example, joint accel-

erations, torques etc.) into the multiple objectives. Potential applications for the presented method include trajectory planning for large scale redundant robots and light-weight space robot arms, to achieve fast but low vibration operations.

Acknowledgment

The work was supported by the Hong Kong Research Grant Council through the project #9040306. The support of the

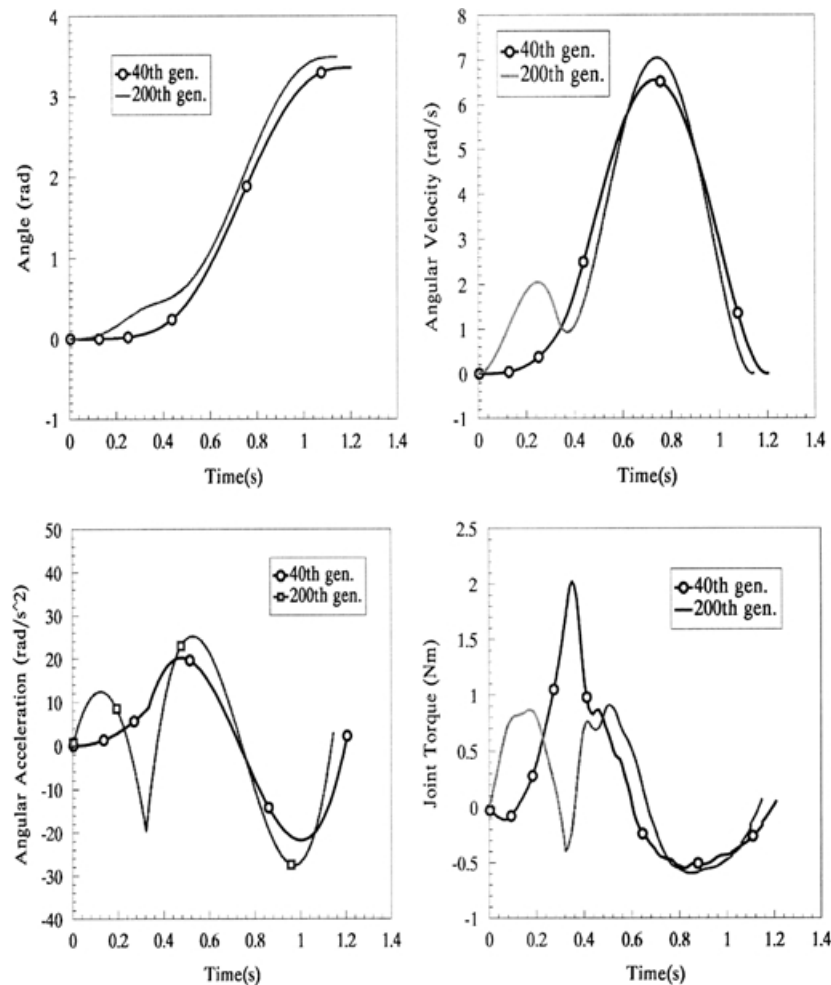


Fig. 14. The angle, angular velocity, angular acceleration and computed joint torque of 1st joint at 40th and 200th generations.

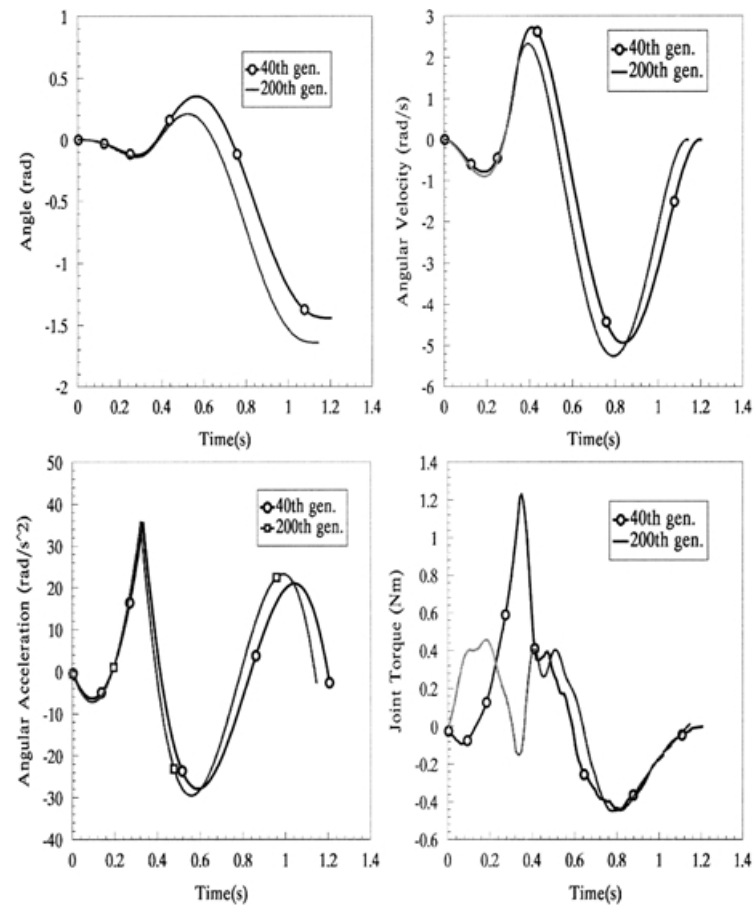


Fig. 15. The angle, angular velocity, angular acceleration and computed joint torque of 2nd joint at 40th and 200th generations.

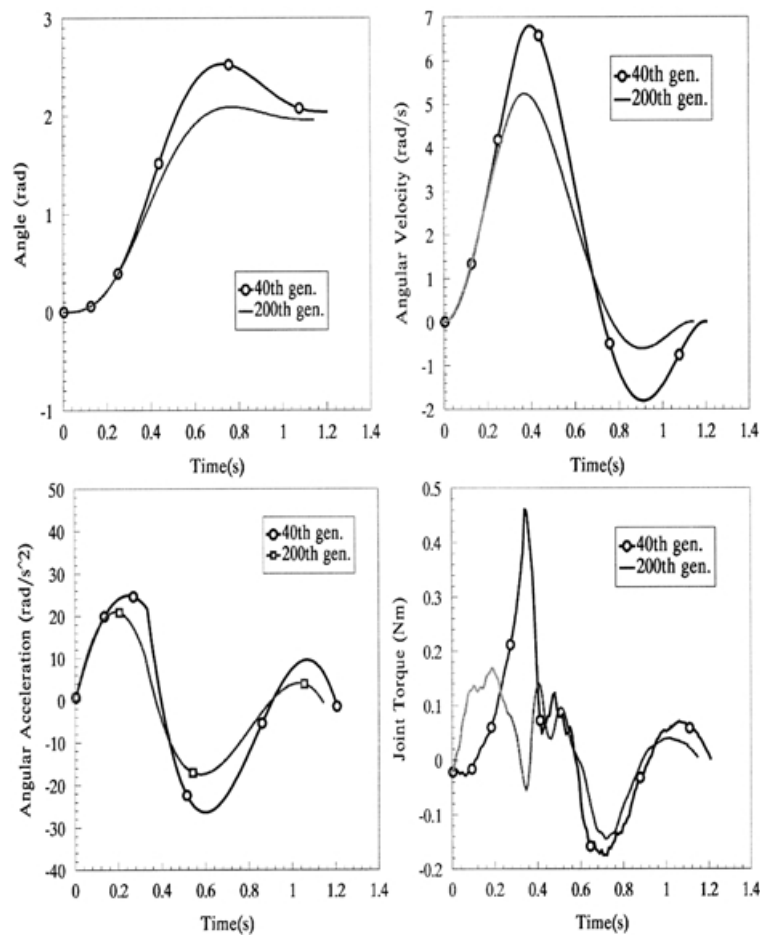


Fig. 16. The angle, angular velocity, angular acceleration and computed joint torque of 3rd joint at 40th and 200th generations.

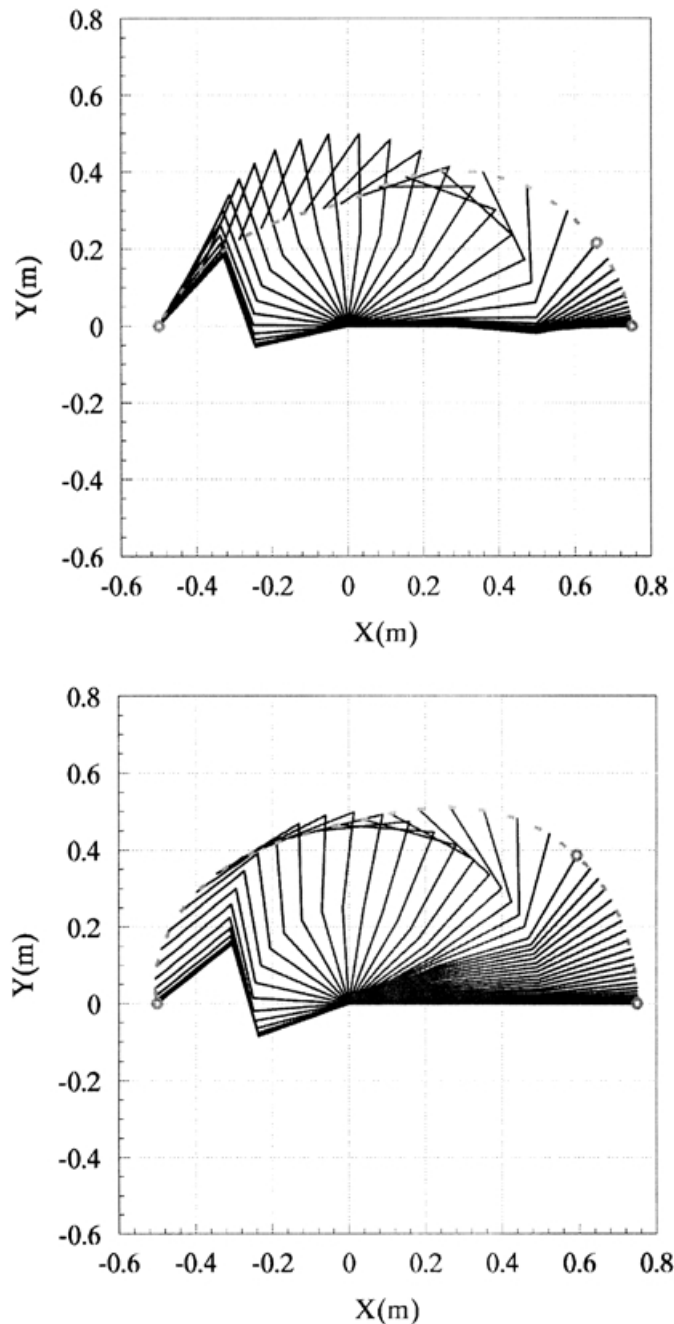


Fig. 17. The configurations and point-to-point path of FRM at 40th generation (above) and 200th generation (below), respectively.

Alexander von Humboldt Foundation is greatly appreciated by the first author. We also thank D. L. Carroll for his GA driver.

References

1. K. Desoyer, P. Kopacek, P. Lugner and I. Troch, "Flexible robot - A survey," *Proc. IFAC*, Vienna, Austria (1986) pp. 23-34.
2. P. E. Gaultier and W. L. Cleghorn, "Modeling of flexible manipulator dynamics: A literature survey," *1st Nat. Appl. Mechanism and Robot Conference*, Cincinnati, OH (1989) pp. 2c-3.1-10.
3. W. J. Book, "Modeling, design, and control of flexible manipulator arms: A tutorial review," *Proc. 29th IEEE Conference on Decision and Control* (1990) pp. 500-506.
4. A. Mohri, P. K. Sarkar and M. Yamamoto, "An efficient motion planning of flexible manipulator along specified path," *Proc. IEEE Int. Conf. On Robotics and Automation* (1998) pp. 1104-1109.
5. N. C. Singer and W. P. Seering, "Using a causal shaping techniques to reduce robot vibration," *IEEE Conference on Robotics and Automation* (1988) pp. 1434-1439.
6. W. E. Singhose, W. P. Seering and N. C. Singer, "Shaping inputs to reduce vibration: a vector diagram approach," *IEEE Proceeding of Conference on Robotics and Automation* (1990) pp. 922-927.
7. S. Choura, S. Jayasuriya and M. A. Medick, "On the modeling, and open-loop control of a rotating thin flexible beam," *Transactions of the ASME, J. of Dynamic Systems, Measurement, and Control* **113**, 26-33 (1991).
8. K. L. Hillsley and S. Yurkovich, "Vibration control of a two link flexible robot," *IEEE Proceeding of Conference on Robotics and Automation* (1991) pp. 2121-2126.
9. D. N. Nenchev, "Redundancy resolution through local optimization: A review," *J. Robotic Systems* **6**, No. 6, 769-798 (1989).
10. B. Siciliano, "Kinematic control of redundant robot manipulators: A tutorial," *J. Intelligent and Robotic Systems* **3**, 201-212 (1990).
11. L. A. Nguyen, I. D. Walker and R. J. P. Defigueiredo, "Dynamic control of flexible kinematically redundant robot manipulators," *IEEE Transactions on Robotics and Automation* **8**, No. 6, 759-767 (1992).
12. S. G. Yue, "Redundant robot manipulators with joints and link flexibility I: dynamic motion planning for minimum end effector deformation," *Mechanism and Machine Theory* **33**, Nos. 1/2, 103-113 (1998).
13. S. J. Kim and Y. S. Park, "Self-motion utilization for reducing vibration of a structurally flexible redundant robot manipulator system," *Robotica* **16**, 669-677 (1998).
14. R. D. Schraft, J. G. Neugebauer and A. Meißner, "Innovative offline-programming method to facilitate large redundant robot operation on free-form geometries," *IFR 29th International Symposium on Robotics (ISR '98)*, 27th April to 1st May, 1998, Birmingham, UK (1998) pp. 109-114.
15. E. Westkämper, R. D. Schraft, M. Schweizer, T. F. Herkommer and A. Meißner, "Task-oriented programming of large redundant robot motion," *Robotics and Computer-Integrated Manufacturing* **14**(5/6), 363-375 (1998).
16. D. B. Fogel, "An introduction to simulated evolutionary optimization," *IEEE Trans. On Neural Networks* **5**(1), 3-14 (1994).
17. D. E. Goldberg, *Genetic Algorithms in Search, Optimization and Machine Learning* (Addison-Wesley, Reading, Mass., 1989).
18. N. Kubota, T. Arakawa, T. Fukuda and K. Shimojima, "Trajectory generation for redundant manipulator using virus evolutionary genetic algorithm," *IEEE Proc. Int. Conf. Robotics and Automation* (1997) pp. 205-210.
19. S. D. Sun, A.S. Morris and A. M. S. Zalazala, "Trajectory planning of multiple coordinating robots using genetic algorithms," *Robotica* **14** (1996) pp. 227-234.
20. S. G. Yue, Y. Q. Yu and S. X. Bai, "Flexible rotor beam element for robot manipulators with link and joint flexibility," *Mechanism and Machine Theory* **32**(2), 209-219 (1997).
21. J. J. Craig, *Introduction to Robotics Mechanics and Control* (Addison-Wesley Publishing Company, USA, 1986).

Point trajectory planning of flexible redundant robot manipulators using genetic algorithms

Yue, Shigang

2002

<http://hdl.handle.net/10179/9683>

22/04/2023 - Downloaded from MASSEY RESEARCH ONLINE